to $^7F_2$ manifold, 0.08 nm, is of the same order of magnitude as transitions often observed in transparent inorganic crystalline compounds.[1] This situation makes fluorescence spectroscopy an extremely useful tool for the elucidation of the structures and purities of appropriate rare-earth chelate compounds. Any irregularities in the synthesis method which may result in a crystallographically impure compound, undetectable by elemental analysis, are exposed by the appearance of the fluorescence spectrum in terms of broadened features and unrecognizable peaks.

The descent in symmetry with increasing size of the alkali metal counterion suggests that still larger cations should exhibit low symmetry. Previous investigations of this anion's solid compounds where large organic counterions have been employed have assigned point symmetries of C_{2v} or lower.[10] Also, when the assignment of point symmetry was performed on the piperidinium compound dissolved in a 3:1 mixture of ethanol and methanol, or a 4:1 mixture of the previous solvent and dimethylformamide, the resultant symmetry assignments were D_{2d} and C_{4v}, respectively.[6] All of the above observations seem to be consistent with the view of a highly symmetric anion being distorted to a varying extent due to the size of the counterion. A descent in symmetry with increasing cation size in the solid compounds could be expected as a result of the anion's response to crystal packing.

---

(10) Nugent, L. J.; Bhaumik, M. L.; George, S.; Lee, S. M. *J. Chem. Phys.* **1964**, *41*, 1305.

Contribution from the Department of Chemistry, University of Winnipeg, Winnipeg, Manitoba, Canada R3B 2E9, and Department of Chemistry and Biochemistry, University of Windsor, Windsor, Ontario, Canada N9B 3P4

Synthesis and Reaction Chemistry of the Coordinatively Unsaturated Heterobimetallic Complexes $(CO)_3(PPh_3)Fe(\mu\text{-}PCy_2)Rh(PPh_3)(CO)$ and $(CO)_4Fe(\mu\text{-}PCy_2)Rh(1,5\text{-}COD)$. Crystal and Molecular Structure of $(CO)_3(PPh_3)Fe(\mu\text{-}PCy_2)Rh(PPh_3)(CO)$

Hilary A. Jenkins,[†] Stephen J. Loeb,[*,†] and Douglas W. Stephan[‡]

Received June 30, 1988

Reactions of $Li[Fe(CO)_4(PCy_2)]$ with *trans*-$RhCl(CO)(PPh_3)_2$ and $[RhCl(1,5\text{-}COD)]_2$ result in the formation of the μ-PCy_2 complexes $(CO)_3(PPh_3)Fe(\mu\text{-}PCy_2)Rh(PPh_3)(CO)$ (**2**) and $(CO)_4Fe(\mu\text{-}PCy_2)Rh(1,5\text{-}COD)$ (**3**), respectively. These complexes are identified by $^{31}P\{^1H\}$ NMR and infrared spectroscopy, and **2** has been further characterized by a single-crystal X-ray diffraction study. It crystallizes in the space group $P2_1/c$ with $a = 23.746$ (3) Å, $b = 10.414$ (2) Å, $c = 19.823$ (3) Å, $\beta = 100.91$ (1)°, $V = 4813$ (1) Å^3, and $Z = 4$. The structure was refined to final $R = 6.85\%$ and $R_w = 7.74\%$ for 5041 reflections with $F_o^2 > 3\sigma(F_o^2)$. The Fe atom has trigonal-bipyramidal geometry, coordinating to the bridging PCy_2 group, one PPh_3 ligand, and three CO groups. The Rh atom has a distorted-square-planar geometry coordinating to the bridging PCy_2 group, one molecule of PPh_3, one CO group, and the Fe atom. The Fe-Rh distance is 2.660 (1) Å, implying a metal-metal interaction, and one of the CO groups on the Fe atom is semibridging to the Rh atom. **2** reacts with CO to give the products $(CO)_3(PPh_3)Fe(\mu\text{-}PCy_2)Rh(PPh_3)(CO_2)$ (**4**) and $(CO)_4Fe(\mu\text{-}PCy_2)Rh(PPh_3)(CO)_2$ (**5**) and with PEt_3 to yield $(CO)_4Fe(\mu\text{-}PCy_2)Rh(PPh_3)(CO)$ (**6**), $(CO)_4Fe(\mu\text{-}PCy_2)Rh(PEt_3)(CO)$ (**7**), $(CO)_4Fe(\mu\text{-}PCy_2)Rh(PPh_3)(PEt_3)$ (**8**), and $(CO)_3(PPh_3)Fe(\mu\text{-}PCy_2)Rh(PEt_3)(CO)$ (**9**). **3** easily loses 1,5-COD under an atmosphere of CO(g) to yield $(CO)_4Fe(\mu\text{-}PCy_2)Rh(CO)_x$ ($x = 1$-3). These reaction products (**4**-**9**) were identified in solution only, by $^{31}P\{^1H\}$ NMR.

Introduction

The diorganophosphide group (PR_2) has shown great versatility as a bridging ligand, and it is particularly suited for the synthesis of heterobimetallic complexes.[1] Although numerous studies have produced a variety of interesting metal combinations,[2-12] there are only a limited number of heterobimetallic complexes that contain easily displaced ligands[13-16] or coordinatively unsaturated metal centers[2,15,16] of the type usually found in reactive mononuclear species.

Our approach has been to employ sterically demanding dicyclohexylphosphido groups in an attempt to create heterobimetallic complexes containing one or both metals with a low coordination number. This is analogous to the use of bulky trialkylphosphines to create sites of coordinative unsaturation in mononuclear complexes.[17] Initially, we focused on complexes employing two dicyclohexylphosphido bridging ligands in order to maximize the steric effects of these groups. The resulting complexes, which linked Mo and W to Ni, Pd, or Pt, exhibited steric crowding at the metal sites, but this did not translate into increased chemical reactivity.[10] In fact, our conclusion was that the bulky phosphide ligands simply acted to shield the metal centers, resulting in relatively unreactive complexes. In this paper, we have taken the approach that a single bridging unit should lessen this steric shielding and the presence of more exposed metal centers may lead to increased chemical reactivity. The complexes described in this paper contain an Fe center and a coordinatively unsaturated Rh center linked by a *single* dicyclohexylphosphido bridge. Some simple reaction chemistry is described as well as

---

[†] University of Winnipeg.

[‡] University of Windsor.

(1) Roberts, D. A.; Geoffroy, G. L. In *Comprehensive Organometallic Chemistry*; Wilkinson, G., Stone, F. G. A., Abel, E., Eds.; Pergamon: Oxford, England, 1982; Chapter 40.

(2) Roberts, D. A.; Steinmetz, G. R.; Breen, M. J.; Shulman, P. M.; Morrison, E. D.; Duttera, M. R.; De Brosse, C. W.; Whittle, R. R.; Geoffroy, G. L. *Organometallics* **1983**, *2*, 846-855.

(3) Morrison, E. D.; Harley, E. D.; Marcelli, M. A.; Geoffroy, G. L.; Rheingold, A. L.; Fultz, W. C. *Organometallics* **1984**, *3*, 1407-1413.

(4) Mercer, W. C.; Whittle, R. R.; Burkhardt, E. W.; Geoffroy, G. L. *Organometallics* **1985**, *4*, 68-74.

(5) Ritchy, J. M.; Zozulin, A. J.; Wrobleski, D. A.; Ryan, R. R.; Wasserman, H. J.; Moody, D. C.; Paine, R. T. *J. Am. Chem. Soc.* **1985**, *107*, 501-503.

(6) Targos, T. S.; Rosen, R. P.; Whittle, R. R.; Geoffroy, G. L. *Inorg. Chem.* **1985**, *24*, 1375-1379.

(7) Gelmini, L.; Matassa, L. C.; Stephan, D. W. *Inorg. Chem.* **1985**, *24*, 2585-2588.

(8) Geoffroy, G. L.; Rosenberg, S.; Shulman, P. M.; Whittle, R. R. *J. Am. Chem. Soc.* **1984**, *106*, 1519-1521.

(9) Rosenberg, S.; Lockledge, S. P.; Geoffroy, G. L. *Organometallics* **1986**, *5*, 2517-2522.

(10) Loeb, S. J.; Taylor, H. A.; Gelmini, L.; Stephan, D. W. *Inorg. Chem.* **1986**, *25*, 1977-1982.

(11) Shulman, P. M.; Burkhardt, E. D.; Lundquist, E. G.; Pilato, R. S.; Geoffroy, G. L. *Organometallics* **1987**, *6*, 101-109.

(12) Baker, R. T.; Tulip, T. H. *Organometallics* **1986**, *5*, 839-845.

(13) Chandler, D. J.; Jones, R. A.; Stuart, A. L.; Wright, T. C. *Organometallics* **1984**, *3*, 1830-1838.

(14) Rosenberg, S.; Mahoney, W. S.; Mayes, J. M.; Geoffroy, G. L.; Rheingold, A. L. *Organometallics* **1986**, *5*, 1065-1071.

(15) Arif, A. M.; Chandler, D. J.; Jones, R. A. *Organometallics* **1987**, *6*, 506-512.

(16) Arif, A. M.; Chandler, D. J.; Jones, R. A. *Inorg. Chem.* **1987**, *26*, 1780-1784.

0020-1669/89/1328-1998$01.50/0

the crystal and molecular structure of the FeRh complex $(CO)_3(PPh_3)Fe(\mu\text{-}PCy_2)Rh(PPh_3)(CO)$.

Experimental Section

trans-$RhCl(CO)(PPh_3)_2$ and $[RhCl(1,5\text{-}COD)]_2$ (COD = cyclooctadiene) were prepared by the literature methods.[18,19] $Fe_2(CO)_9$, $RhCl_3 \cdot xH_2O$, PCy_2H (Strem), PPh_3, PEt_3, and *n*-BuLi (Aldrich) were purchased and used as received. THF (tetrahydrofuran), toluene, and *n*-hexane were dried by distillation from Na–benzophenone ketyl under N_2. All reactions were conducted under an atmosphere of dry N_2 by using standard Schlenk techniques.

$^{31}P\{^1H\}$ NMR spectra were obtained at 121.5 MHz on a Bruker AM300 spectrometer using deuterated solvents as locks. Phosphorus chemical shifts were measured relative to external 85% H_3PO_4 with positive shifts downfield. Infrared spectra were recorded on a Perkin-Elmer 781 grating spectrometer.

Preparation of $Fe(CO)_4(PCy_2H)$ (1). PCy_2H (2.84 mL, 13.75 mmol) was added to a suspension of $Fe_2(CO)_9$ (5.0 g, 13.75 mmol) in toluene (50 mL). The brown solution was stirred for 24 h at 35 °C, during which time the $Fe_2(CO)_9$ completely dissolved. The volatiles were removed in vacuo, leaving a viscous brown oil. The residue was extracted with *n*-heptane (30 mL), and the extracts were filtered and cooled to −20 °C for 12 h. This yielded brown crystals (4.14 g, 82%). Anal. Calcd for $C_{16}H_{25}O_4PFe$: C, 52.47; H, 6.37. Found: C, 51.06; H, 6.21. ^{31}P NMR: δ 54.6 ($^1J_{PH}$ = 344.3 Hz).

Preparation of $(CO)_3(PPh_3)Fe(\mu\text{-}PCy_2)Rh(PPh_3)(CO)$ (2). *n*-Butyllithium (0.935 mL, 1.45 mmol of a 1.55 M solution in hexane) was added via syringe to a brown solution of $Fe(CO)_4(PCy_2H)$ (0.530 g, 1.45 mmol) in THF (10 mL). This solution was stirred for 10 min and then added dropwise to a yellow slurry of *trans*-$RhCl(CO)(PPh_3)_2$ (1.00 g, 1.45 mmol) in THF (10 mL) at 23 °C. The resulting dark orange-brown solution was stirred for 24 h at room temperature and the solvent removed in vacuo. The remaining dark brown solid was extracted with toluene (4 × 10 mL) and the volume reduced to 10 mL. Cooling to −20 °C for 24 h yielded orange microcrystals of the product (0.94 g, 65%). $^{13}C\{^1H\}$ NMR (−80 °C, CD_2Cl_2): δ 217.5, 213.7 (br, Fe–CO), 198.9 (br t, Rh–CO). Anal. Calcd for $C_{52}H_{52}O_4P_3FeRh$: C, 62.87; H, 5.29. Found: C, 62.60; H, 5.29.

Preparation of $(CO)_4Fe(\mu\text{-}PCy_2)Rh(1,5\text{-}COD)$ (3). *n*-Butyllithium (1.52 mL, 2.43 mmol of a 1.6 M solution in hexane) was added via syringe to a brown solution of $Fe(CO)_4(PCy_2H)$ (0.89 g, 2.43 mmol) in THF (5 mL). The resulting dark brown solution was stirred at room temperature for 10 min and then cooled to −10 °C. This cooled solution was then added dropwise to an orange solution of $[RhCl(1,5\text{-}COD)]_2$ (0.60 g, 1.22 mmol) in THF (5 mL). An immediate color change was observed from orange to an intense dark orange-brown. Stirring was continued for 3 h at −10 °C, the solution taken to dryness in vacuo, and the resulting brown oil extracted with toluene (3 × 5 mL). The solution was filtered and the volume reduced to 5 mL. After the solution was cooled at −20 °C for 48 h, brown microcrystalline material was isolated (0.46 g, 50%). $^{13}C\{^1H\}$ NMR (CD_2Cl_2): δ 215.4 (br, CO), δ 87.9, 86.9 (br, CH, COD), 28.6 (CH_2, COD). ^1H NMR (CD_2Cl_2): δ 5.41, 4.78 (br s, 4 H, COD), 2.22 (br s, 8 H, COD), 0.95–1.80 (br m, 22 H, Cy). A satisfactory elemental analysis could not be obtained.

Reactions of $(CO)_3(PPh_3)Fe(\mu\text{-}PCy_2)Rh(PPh_3)(CO)$ with CO. $(CO)_3(PPh_3)Fe(\mu\text{-}PCy_2)Rh(PPh_3)(CO)$ (2; 0.050 g, 0.050 mmol) was dissolved in toluene-d_8. CO(g) was introduced as the atmosphere in place of N_2(g) and the resulting solution stirred for 30 min. A 3-mL sample of the solution was then removed and the $^{31}P\{^1H\}$ NMR spectrum recorded under an atmosphere (1 atm) of CO(g).

Reaction of $(CO)_3(PPh_3)Fe(\mu\text{-}PCy_2)Rh(PPh_3)(CO)$ with PEt_3. $(CO)_3(PPh_3)Fe(\mu\text{-}PCy_2)Rh(PPh_3)(CO)$ (2; 0.050 g, 0.050 mmol) was dissolved in toluene-d_8 (5 mL). PEt_3 (0.0070 mL, 0.050 mmol) was then added via microsyringe and the resulting solution stirred for 30 min. A 3-mL sample of the solution was removed and the $^{31}P\{^1H\}$ NMR spectrum recorded.

Reaction of $(CO)_4Fe(\mu\text{-}PCy_2)Rh(1,5\text{-}COD)$ with CO. $(CO)_4Fe(\mu\text{-}PCy_2)Rh(1,5\text{-}COD)$ (3; 0.050 g, 0.132 mmol) was dissolved in toluene-d_8 and CO(g) introduced in place of the N_2(g) atmosphere. The resulting orange-brown solution showed a very slight color change to dark yellow-brown, and the solution was stirred for 3 h with no further color variation. A 3-mL sample was removed and the $^{31}P\{^1H\}$ NMR spectrum recorded under an atmosphere of CO(g) (1 atm).

X-ray Diffraction Study of 2. Orange-brown crystals of 2 were obtained by recrystallization from toluene at −20 °C. Diffraction experiments were performed on a four-circle Syntex $P2_1$ diffractometer with graphite-monochromatized Mo Kα radiation. The initial orientation matrix was obtained from 15 machine-centered reflections selected from rotation photographs. Partial rotation photographs around each axis were consistent with a monoclinic crystal system. Ultimately, 30 high-angle reflections (22° < 2θ < 25°) were used to obtain the final lattice parameters and orientation matrix. Machine parameters, crystal data, and data collection parameters are summarized in Tables I and S-I (Table S-I is in the supplementary material). The observed extinctions were consistent with space group $P2_1/c$. Intensity data ($+h,+k,+l$) were collected in one shell (4.5° < 2θ < 45°). The intensities of three standard reflections were recorded every 197 reflections and showed no statistically significant changes over the duration of the data collection. The data were processed by using the SHELX-76 program package on the computing facilities at the University of Windsor. A total of 6810 reflections were collected, and 5041 unique reflections with $F_o^2 > 3\sigma(F_o^2)$ were used in the refinement. The absorption coefficient was small (μ = 7.17 cm^{-1}), and ψ scans recorded showed no significant absorption effects. Thus, no absorption correction was applied to the data.

Table I. Crystallographic Data for $(CO)_3(PPh_3)Fe(\mu\text{-}PCy_2)Rh(PPh_3)(CO)$ (**2**)

chem formula: $C_{52}H_{52}FeP_3O_4Rh$	fw: 1007.7
a = 23.746 (3) Å	space group: $P2_1/c$
b = 10.414 (2) Å	T = 24 °C
c = 19.823 (3) Å	λ = 0.71069 Å
β = 100.91 (1)°	ρ(calcd) = 1.37 g cm^{-3}
V = 4813 (1) Å^3	μ = 7.17 cm^{-1}
Z = 4	$R(F_o^2)$ = 6.85%
	$R_w(F_o^2)$ = 7.74%

The Rh atom position was determined by using the Patterson method, and the remaining non-hydrogen atoms were located from successive difference Fourier map calculations. Refinement was carried out by using full-matrix least-squares techniques on F, minimizing the function $\sum w(|F_o| - |F_c|)^2$, where $w = 4F_o^2/\sigma^2(F_o^2)$ and F_o and F_c are the observed and calculated structure factors. Atomic scattering factors[20] and anomalous dispersion[21] terms were taken from the usual sources. In the final cycles of refinement, the Rh, Fe, P, O, and carbonyl and cyclohexyl C atoms were assigned anisotropic thermal parameters. The phenyl carbon atoms were constrained to an idealized C_{6h} symmetry with C–C distances of 1.39 Å and assigned isotropic thermal parameters. Fixed H atom contributions were included with C–H distances of 0.95 Å and thermal parameters equal to 1.1 times the isotropic thermal parameter of the bonded C atoms. No H atoms were refined, but all values were updated as refinement continued. This resulted in $R = \sum||F_o| - |F_c|/\sum|F_o|| = 0.0685$ and $R_w = (\sum w(|F_o| - |F_c|)^2/\sum wF_o^2)^{1/2} = 0.0774$ at final convergence.

The Δ/σ values for any parameters in the final cycles were less than 0.001. A final difference Fourier map calculation showed no peaks of chemical significance; the largest was 1.2 e Å^{-3} and was associated with one of the phenyl rings (C61–C66). Atomic positional parameters are summarized in Table II and selected bond distances and angles in Table III. Anisotropic thermal parameters (Table S-II), hydrogen atom parameters (Table S-III), bond distances and angles associated with the cyclohexyl groups (Table S-IV), and values of $10|F_o|$ and $10|F_c|$ (Table S-V) are deposited as supplementary material.

Results

Synthesis and Characterization of 2 and 3. The heterobimetallic FeRh complexes $(CO)_3(PPh_3)Fe(\mu\text{-}PCy_2)Rh(PPh_3)(CO)$ (2) and $(CO)_4Fe(\mu\text{-}PCy_2)Rh(1,5\text{-}COD)$ (3) were prepared by the bridge-assisted synthetic method.[1] This involved the nucleophilic displacement of chloride, from *trans*-$RhCl(CO)(PPh_3)_2$ and $[RhCl(1,5\text{-}COD)]_2$, respectively, by the phosphido group of $Li[Fe(CO)_4(PCy_2)]$ according to eq 1 and 2.

$$\textit{trans}\text{-}RhCl(CO)(PPh_3)_2 + Li[Fe(CO)_4(PCy_2)] \rightarrow (CO)_3(PPh_3)Fe(\mu\text{-}PCy_2)Rh(PPh_3)(CO) + LiCl \quad (1)$$

$$[RhCl(1,5\text{-}COD)]_2 + 2Li[Fe(CO)_4(PCy_2)] \rightarrow 2(CO)_4Fe(\mu\text{-}PCy_2)Rh(1,5\text{-}COD) + 2LiCl \quad (2)$$

The phosphide complex $Li[Fe(CO)_4(PCy_2)]$ was generated in situ by the treatment of $Fe(CO)_4(PCy_2H)$ (1) with *n*-BuLi in THF

---

(17) Tolman, C. A. *Chem. Rev.* **1977**, *77*, 313–348.

(18) Evans, D.; Osborn, J. A.; Wilkinson, G. *Inorg. Synth.* **1968**, *11*, 99–101.

(19) Giordano, G.; Crabtree, R. H. *Inorg. Synth.* **1979**, *19*, 218–220.

(20) Cromer, D. T.; Waber, J. T. *International Tables for X-ray Crystallography*; Kynoch: Birmingham, England, 1974.

(21) (a) Cromer, D. T.; Mann, J. B. *Acta Crystallogr., Sect. A: Cryst. Phys., Diffr., Theor. Gen. Crystallogr.* **1968**, *A24*, 321. (b) *Ibid.* **1968**, *A24*, 390.

Table II. Positional Parameters[a]

atom	*x*	*y*	*z*	atom	*x*	*y*	*z*
Rh	2296 (1)	1379 (1)	−1347 (1)	Fe	3117 (1)	2736 (1)	8239 (1)
P1	1420 (1)	535 (2)	8639 (1)	P2	3902 (1)	3534 (2)	8908 (1)
P3	2292 (1)	2081 (2)	7561 (1)	O1	2656 (4)	410 (8)	100 (4)
O2	2533 (2)	4082 (6)	9228 (3)	O3	3378 (3)	4264 (7)	7097 (3)
O4	3776 (3)	210 (7)	8360 (4)	C1	2535 (4)	827 (9)	9574 (4)
C2	2711 (3)	3453 (8)	8832 (4)	C3	3268 (4)	3652 (8)	7543 (4)
C4	3438 (4)	1194 (9)	8302 (5)	C11	998 (2)	1440 (5)	9175 (3)
C12	1269 (2)	2396 (5)	9611 (3)	C13	969 (2)	3047 (5)	47 (3)
C14	397 (2)	2742 (5)	45 (3)	C15	125 (2)	1786 (5)	9608 (3)
C16	425 (2)	1135 (5)	9173 (3)	C21	880 (3)	369 (4)	7838 (2)
C22	788 (3)	−802 (4)	7493 (2)	C23	391 (3)	−885 (4)	6878 (2)
C24	87 (3)	203 (4)	6608 (2)	C25	180 (3)	1374 (4)	6952 (2)
C26	576 (3)	1457 (4)	7568 (2)	C31	1465 (2)	−1123 (5)	8975 (2)
C32	1913 (2)	−1857 (2)	8816 (2)	C33	1977 (2)	−3136 (5)	9025 (2)
C34	1592 (2)	−3681 (5)	9394 (2)	C35	1144 (2)	−2974 (5)	9554 (2)
C36	1080 (2)	−1668 (5)	9345 (2)	C41	4172 (2)	2639 (6)	9698 (3)
C42	3782 (2)	2367 (6)	123 (3)	C43	3956 (2)	1664 (6)	726 (3)
C44	4521 (2)	1232 (6)	903 (3)	C45	4911 (2)	1504 (6)	478 (3)
C46	4737 (2)	2207 (6)	9876 (3)	C51	4539 (3)	3695 (5)	8500 (3)
C52	4678 (3)	2684 (5)	8099 (3)	C53	5153 (3)	2780 (5)	7783 (3)
C54	5490 (3)	3887 (5)	7867 (3)	C55	5351 (3)	4898 (5)	8268 (3)
C56	4876 (3)	4802 (5)	8584 (3)	C61	3809 (3)	5185 (6)	9193 (2)
C62	3560 (3)	6081 (6)	8703 (2)	C63	3459 (3)	7332 (6)	8903 (2)
C64	3608 (3)	7686 (6)	9593 (2)	C65	3858 (3)	6789 (6)	82 (2)
C66	3958 (3)	5539 (6)	9882 (2)	C71	1752 (3)	3274 (8)	7146 (4)
C72	1591 (4)	4223 (9)	7676 (4)	C73	1110 (4)	5116 (9)	7343 (5)
C74	1245 (5)	5800 (10)	6748 (6)	C75	1411 (5)	4913 (11)	6222 (6)
C76	1895 (4)	3990 (10)	6539 (5)	C81	2315 (4)	909 (8)	6861 (4)
C82	2810 (5)	1100 (10)	6481 (5)	C83	2784 (6)	135 (12)	5902 (6)
C84	2781 (7)	−1194 (12)	6135 (6)	C85	2297 (6)	−1439 (11)	6501 (7)
C86	2329 (5)	−484 (10)	7114 (5)				

[a] Multiplied by 10^4.

and this solution added to a solution of the appropriate Rh complex. Best results were obtained when the preparation of **3** was carried out at −10 °C or cooler. Both complexes are soluble in toluene and *n*-hexane to give intense orange to orange-brown solutions.

The $^{31}P\{^1H\}$ NMR spectral data for **2** and **3** are summarized in Table IV. Complex **2** shows a downfield resonance (δ 167.2 (ddd)) due to the bridging PCy_2 ligand coupled to two different PPh_3 groups ($^2J_{PP}$(Fe) = 23.1 Hz and $^2J_{PP}$(Rh) = 19.4 Hz) and directly to the ^{103}Rh center ($^1J_{PRh}$ = 103.3 Hz). The two different PPh_3 groups are easily distinguished, as the ligand bound to Rh shows direct coupling to the Rh center (δ 34.8, $^1J_{PRh}$ = 200.5 Hz) while the ligand bound to Fe is a simple doublet (δ 78.0). The downfield chemical shift for the μ-PCy_2 ligand is indicative of a phosphido group bridging a metal–metal bond.[22] This correlation has been observed for μ-PPh_2 ligands[23] and also for bulky groups such as μ-P-*t*-Bu_2[24-26] and μ-PCy_2[10,27] and is well supported by X-ray studies. The $^2J_{PP}$ couplings between the bridging group and the terminal PPh_3 ligands support a structure in which the PPh_3 group on Rh is cis to the μ-PCy_2 bridge and the PPh_3 group on Fe is trans to the μ-PCy_2 bridge.[28]

The infrared spectra of **2** in *n*-hexane solution (ν(CO): 2038 w, 1980 s, 1950 s, 1900 w cm^{-1}) and as a Nujol mull (ν(CO): 1991 s, 1980 s, 1896 s, 1842 s cm^{-1}) both show four bands assignable to four CO groups; however, the positions are quite different. The major change appears to be a loss of the highest solution band at 2038 cm^{-1} and the addition of a low band at 1842 cm^{-1} in the solid state. This is explained by the formation of a semibridging CO group in the solid that is not observable in the solution. The solution infrared spectrum showed no solvent dependence, and there was no high-field ^{1}H NMR evidence for an agostic C–H interaction that might provide electron density in lieu of the semibridging CO group. Attempts to identify a semibridging CO group in solution at low temperatures using $^{13}C\{^1H\}$ NMR were unsuccessful, but the presence of this group in the solid state was verified by an X-ray crystallographic study (vide infra).

Thus, the structure of **2** in solution can be formulated as containing an Fe to Rh dative bond and a Rh center that is formally coordinatively unsaturated, while the structure of **2** in the solid state is more appropriately described as containing a semibridging CO group accompanied by a metal–metal bond.

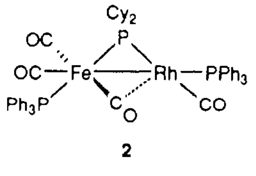

2

The $^{31}P\{^1H\}$ NMR spectrum of **3** shows only a single downfield doublet due to the μ-PCy_2 ligand (δ 142.6, $^1J_{PRh}$ = 128.8 Hz), and this chemical shift is also attributed to the phosphido ligand bridging a metal–metal bond. The infrared spectrum (solution and solid state) shows four bands (ν(CO): 2040 m, 2004 s, 1971 s, 1837 m cm^{-1}) due to the four CO groups that are bonded to Fe. It is likely that ν(CO) at 1837 cm^{-1} is a semibridging CO group since this occurs for **2** in the solid state and was also observed for $(MeCp)(CO)_2Mn(\mu$-P-*t*-$Bu_2)M(1,5$-COD) (M = Rh, Ir)[16] and (CO)(*t*-$Bu_2PH)Fe(\mu$-P-*t*-Bu_2)Rh(1,5-COD).[15] $^{13}C\{^1H\}$ and ^{1}H NMR spectra show resonances due to coordinated 1,5-COD ($^{13}C\{^1H\}$, δ 87.9, 86.9 (CH), 28.6 (CH_2); ^{1}H, δ 5.41, 4.78 (CH),

---

(22) (a) Peterson, J. L.; Stewart, R. P., Jr. *Inorg. Chem.* **1980**, *19*, 186–191. (b) Carty, A. J.; MacLaughlin, S. A.; Taylor, N. J. *J. Organomet. Chem.* **1981**, *204*, C27–C29. (c) Carty, A. J. *Catalytic Aspects of Metal Phosphine Complexes*; Advances in Chemistry 196; American Chemical Society: Washington, DC, 1982; p 163. (d) Garrou, P. E. *Chem. Rev.* **1981**, *81*, 229–266.

(23) Carty, A. J.; MacLaughlin, S. A.; Nuccarione, D. In *Phosphorus-31 NMR Spectroscopy in Stereochemical Analysis*; Verkade, J. G., Quinn, L. D., Eds.; VCH: Deerfield Beach, FL, 1987; Chapter 16, p 559, and references therein.

(24) Arif, A. M.; Jones, R. A.; Seeberger, M. H.; Whittlesey, B. R.; Wright, T. C. *Inorg. Chem.* **1986**, *25*, 3943–3949 and references 6–11 therein.

(25) Arif, A. M.; Heaton, D. E.; Jones, R. A.; Nunn, C. M. *Inorg. Chem.* **1987**, *26*, 4228–4231.

(26) Arif, A. M.; Heaton, D. E.; Jones, R. A.; Kidd, K. B.; Wright, T. C.; Whittlesey, B. R.; Atwood, J. L.; Hunter, W. E.; Zhang, H. *Inorg. Chem.* **1987**, *26*, 4065–4073.

(27) Albright, T. A.; Kang, S.-K.; Arif, A. M.; Bard, A. J.; Jones, R. A.; Leland, J. K.; Schwab, S. T. *Inorg. Chem.* **1988**, *27*, 1246–1253.

(28) Nixon, J. F.; Pidcock, A. *Annu. Rev. NMR Spectrosc.* **1969**, *2*, 345

Table III. Selected Bond Distances and Angles

	Distances (Å)		
Rh–Fe	2.660 (1)	Fe–P2	2.235 (2)
Rh–P1	2.254 (2)	Fe–P3	2.259 (2)
Rh–P3	2.282 (2)	Fe–C2	1.815 (9)
Rh–C1	1.896 (8)	Fe–C3	1.769 (9)
Rh–C2	2.373 (8)	Fe–C4	1.773 (9)
P1–C11	1.850 (6)	P2–C41	1.832 (6)
P1–C21	1.850 (5)	P2–C51	1.853 (8)
P1–C31	1.847 (5)	P2–C61	1.836 (6)
P3–C71	1.861 (8)	C1–O1	1.12 (1)
P3–C81	1.857 (8)	C2–O2	1.16 (1)
C3–O3	1.16 (1)	C4–O4	1.17 (1)
	Angles (deg)		
Fe–Rh–P1	158.8 (1)	Rh–Fe–P2	126.4 (1)
Fe–Rh–P3	53.7 (1)	Rh–Fe–P3	54.5 (1)
Fe–Rh–C1	110.7 (3)	Rh–Fe–C2	60.6 (3)
Fe–Rh–C2	41.8 (2)	Rh–Fe–C3	142.8 (3)
P1–Rh–P3	106.0 (1)	Rh–Fe–C4	80.1 (3)
P1–Rh–C1	90.1 (3)	P2–Fe–P3	175.6 (1)
P1–Rh–C2	135.5 (2)	P2–Fe–C2	87.0 (2)
P3–Rh–C1	163.0 (3)	P2–Fe–C3	89.5 (3)
P3–Rh–C2	77.1 (2)	P2–Fe–C4	89.7 (3)
C1–Rh–C2	95.2 (3)	C2–Fe–C3	119.6 (4)
Rh–P1–C11	113.2 (2)	C2–Fe–C4	127.0 (4)
Rh–C1–C21	122.3 (2)	C3–Fe–C4	113.3 (4)
Rh–C1–C31	111.7 (2)	Fe–P2–C41	115.9 (2)
C11–P1–C21	100.3 (2)	Fe–P2–C51	115.7 (2)
C11–P1–C31	105.7 (3)	Fe–P2–C61	113.3 (2)
C21–P1–C31	101.9 (2)	C41–P2–C51	103.7 (3)
Rh–P3–C71	120.8 (3)	C41–P2–C61	104.9 (3)
Rh–P3–C81	120.1 (3)	C51–P2–C61	101.8 (3)
C71–P3–C81	102.9 (3)	Fe–P3–C71	120.6 (3)
Rh–C1–O1	174.3 (8)	Fe–P3–C81	119.9 (3)
Rh–C2–O2	114.8 (6)	Fe–C2–O2	167.2 (7)
Fe–C3–O3	178.5 (7)	Fe–C4–O4	176.4 (8)
P1–C11–C12	118.9 (4)	P2–C41–C42	117.0 (4)
P1–C11–C16	121.1 (4)	P2–C41–C46	122.9 (5)
P1–C21–C22	121.4 (4)	P2–C51–C52	118.7 (5)
P1–C21–C26	118.5 (6)	P2–C51–C56	121.3 (5)
P1–C31–C32	115.2 (4)	P2–C61–C62	118.2 (3)
P1–C31–C36	124.8 (4)	P2–C61–C66	121.7 (4)
P3–C71–C72	111.5 (5)	P3–C81–C82	114.7 (6)
P3–C71–C76	116.3 (6)	P3–C81–C82	112.3 (6)

2.22 (CH_2)). The most probable structure for **3** is an $Fe(CO)_4$ fragment and a Rh(1,5-COD) fragment bridged by the μ-PCy_2 ligand and containing an Fe–Rh bond and a semibridging CO group, analogous to the solid-state structure of **2**.

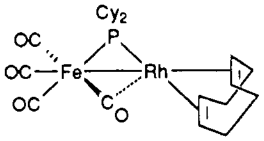

3

Crystal and Molecular Structure of 2. A perspective view of **2** giving the atom-numbering scheme is shown in Figure 1, and a representation of the inner coordination sphere of the molecule is shown in Figure 2. The unit cell contains four discrete molecules of **2**. The closest intermolecular nonbonded contact is 2.443 Å between H15 and H36. Complete listings of interatomic distances and angles may be found in Tables III and S-III.

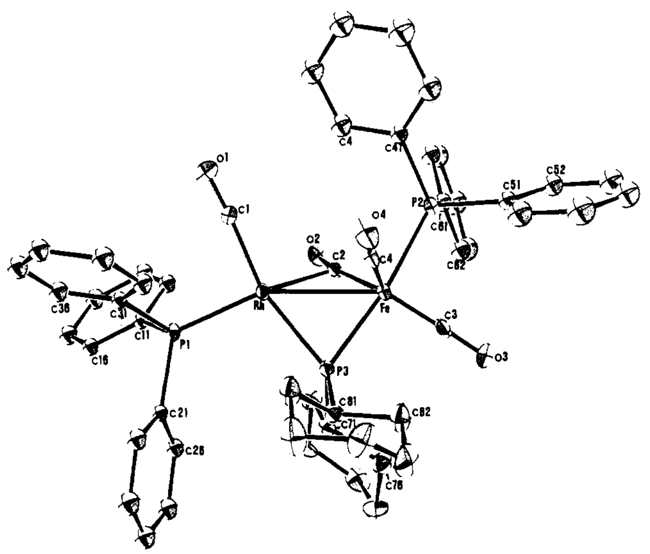

Figure 1. Perspective ORTEP drawing of $(CO)_3(PPh_3)Fe(\mu\text{-}PCy_2)Rh(PPh_3)(CO)$ (**2**) showing the numbering scheme. The numbering of phenyl and cyclohexyl ring carbon atoms starts at the atom bound to phosphorus: 20% thermal ellipsoids are shown.

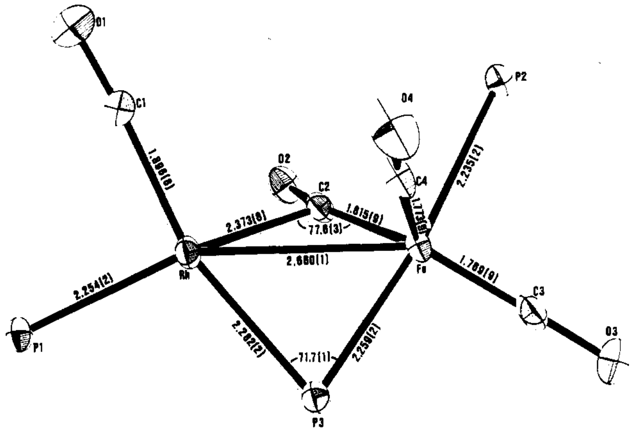

Figure 2. Perspective ORTEP drawing of $(CO)_3(PPh_3)Fe(\mu\text{-}PCy_2)Rh(PPh_3)(CO)$ (**2**) with only the first carbon atoms of each phenyl and cyclohexyl ring shown. Some relevant bonding parameters are shown.

The overall geometry for this bimetallic complex is a combination of the individual coordination geometries of the Fe and Rh atoms. The Fe atom is bonded to two phosphorus atoms (P2 and P3) and three carbonyl carbon atoms (C2, C3, and C4). The three CO groups form a trigonal plane with typical Fe–C distances

Table IV. $^{31}P\{^1H\}$ NMR Spectral Data[a]

complex	$\delta(\mu\text{-}PCy_2)$	$\delta(PPh_3\text{–}Fe)$	$\delta(PR_3\text{–}Rh)$	$^2J_{PP}(\mu\text{-}Fe)$, Hz	$^2J_{PP}(\mu\text{-}Rh)$, Hz	$^1J_{PRh}(\mu)$, Hz	$^1J_{PRh}(Rh)$, Hz
$(CO)_3(PPh_3)Fe(\mu\text{-}PCy_2)Rh(PPh_3)(CO)$ (**2**)	167.2 (ddd)	78.0 (d)	34.8 (dd)	23.1	19.4	103.3	200.5
$(CO)_4Fe(\mu\text{-}PCy_2)Rh(1,5\text{-}COD)$ (**3**)	142.6 (d)					128.8	
$(CO)_3(PPh_3)Fe(\mu\text{-}PCy_2)Rh(PPh_3)(CO)_2$ (**4**)	196.6 (ddd)	77.4 (d)	36.0 (dd)	21.9	187.1	80.1	100.8
$(CO)_4Fe(\mu\text{-}PCy_2)Rh(PPh_3)(CO)_2$ (**5**)	189.8 (dd)		38.8 (dd)		199.3	82.6	103.3
$(CO)_4Fe(\mu\text{-}PCy_2)Rh(PPh_3)(CO)$ (**6**)	177.4 (dd)		31.5 (dd)		212.2	98.4	136.0
$(CO)_4Fe(\mu\text{-}PCy_2)Rh(PEt_3)(CO)$ (**7**)	162.2 (dd)		18.3 (dd)		214.8	94.8	136.8
$(CO)_4Fe(\mu\text{-}PCy_2)Rh(PEt_3)(PPh_3)$ (**8**)	183.9 (ddd)		30.2 (ddd, PPh_3) 8.0 (ddd, PEt_3)	29.1[b]	14.6 (PEt_3) 212.1 (PPh_3)	104.4	199.1 (PPh_3) 134.9 (PEt_3)
$(CO)_3(PPh_3)Fe(\mu\text{-}PCy_2)Rh(PEt_3)(CO)$ (**9**)	157.0 (ddd)	80.4 (d)	21.2 (dd)	20.0	210.9	94.8	134.9
$(CO)_4Fe(\mu\text{-}PCy_2)Rh(CO)_2$ (**10**)	172.9 (d)					103.3	
$(CO)_4Fe(\mu\text{-}PCy_2)Rh(CO)_3$ (**11**)	217.5 (d)					89.8	
$(CO)_4Fe(\mu\text{-}PCy_2)Rh(CO)_4$ (**12**)	16.2 (d)					117.9	

[a] Recorded in toluene solution. [b] $^2J_{PP}(PPh_3\text{–}PEt_3)$. [c] Abbrevation: d = doublet.

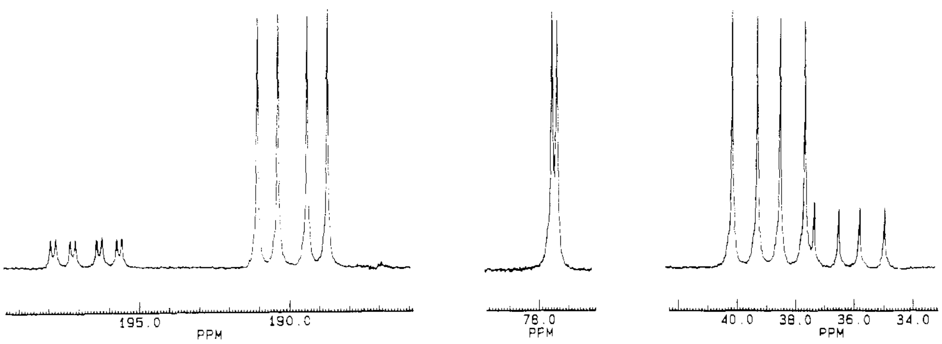

Figure 3. $^{31}P\{^1H\}$ NMR spectrum of $(CO)_3(PPh_3)Fe(\mu\text{-}PCy_2)Rh(PPh_3)(CO)$ (**2**) under CO(g) at 240 K, showing the formation of adducts $(CO)_3(PPh_3)Fe(\mu\text{-}PCy_2)Rh(PPh_3)(CO)_2$ (**4**) and $(CO)_4Fe(\mu\text{-}PCy_2)Rh(PPh_3)(CO)_2$ (**5**).

averaging 1.79 (2) Å and an average OC–Fe–CO bond angle of 120.0 (7)°. The largest deviation from a least-squares trigonal plane for the $Fe(CO)_3$ fragment is 0.03 Å for Fe. The Fe–P2 and Fe–P3 distances are 2.235 (2) and 2.259 (2) Å, respectively, and the P2–Fe–P3 angle is 175.6 (1)° with the CO groups tipped slightly toward the less crowded PPh_3 site; the average OC–Fe–P3 angle is 88.7 (5)°. This is consistent with trigonal-bipyramidal geometry for Fe if we neglect the FeRh interaction. The Rh atom is bonded to two phosphorus atoms (P1 and P3), a carbonyl carbon atom (C1), and the Fe atom. The Rh–P1 and Rh–P3 distances are 2.254 (2) and 2.282 (2) Å, respectively, with a P1–Rh–P3 bond angle of 106.0 (1)° reflecting the cis orientation of these two large groups. The Rh–C1 distance is 1.896 (8) Å, and the bond angles of 90.1 (3)° to the cis PPh_3 ligand and 163.0 (3)° to the trans μ-PCy_2 group are consistent with a square-planar geometry at Rh. The fourth site of the square-planar geometry is quite distorted, however, as the P3–Rh–Fe and C1–Rh–Fe bond angles are 110.7 (3) and 53.7 (1)°, respectively. A least-squares plane calculation for the Rh–Fe–P1–P3–C1 atoms shows a maximum deviation of 0.30 Å for Rh, and we conclude that the best description of the geometry at the Rh center is distorted square planar.

The Fe–Rh bond distance of 2.660 (1) Å is in the range of 2.563–2.690 Å found for other phosphido-bridged FeRh complexes[29] and compares well with that recently determined for $(CO)_3(t\text{-}Bu_2PH)Fe(\mu\text{-}P\text{-}t\text{-}Bu_2)Rh(1,5\text{-}COD)$.[15] An interesting feature of **2** is the presence of a semibridging CO group in the solid-state structure that does not appear to be present in solution. The Fe–C2–O2 angle of 167.2 (7)° is significantly different from the other Fe–C–O angles in **2** (average 177.5 (10)°) and in the range generally found for semibridging CO groups.[30-34] The Rh–C2 distance of 2.373 (8) Å is long but comparable to that of other semibridging CO groups on Rh, for example 2.40 (1) Å for $(MeCp)(CO)_2Mn(\mu\text{-}P\text{-}t\text{-}Bu_2)Rh(1,5\text{-}COD)$[16] and 2.29 (2) Å for $(CO)_3(t\text{-}Bu_2PH)Fe(\mu\text{-}P\text{-}t\text{-}Bu_2)Rh(1,5\text{-}COD)$.[15]

The major steric effect of having a bulky PCy_2 bridging ligand cis to a relatively large ancillary PPh_3 ligand is to open up the P1–Rh–P3 bond angle to 106.0 (1)°, which is considerably larger than the expected 90° for square-planar geometry.

Reaction Chemistry of 2 and 3. Since both **2** and **3** are coordinatively unsaturated at the formally Rh(I) center, we chose to study some simple addition reactions. In particular, the formation of adducts with use of two-electron donors such as CO and PEt_3 was studied.

This is not as straightforward as for mononuclear complexes since the presence of a dative bond from Fe to Rh makes it possible for adduct formation at Rh as well as substitution at Rh for the FeRh bond.[4] The possibility of ligand rearrangement reactions is also higher since ligand transfer between metals may be facile, particularly for CO:

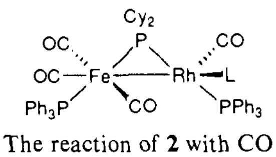

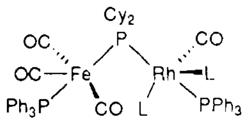

The reaction of **2** with CO was monitored via $^{31}P\{^1H\}$ NMR by recording the spectrum under an atmosphere of CO(g). The low-temperature spectrum showed the formation of two products, **4** and **5** (Figure 3). Both complexes are coordinatively saturated

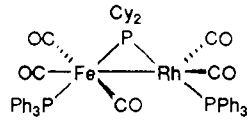

4

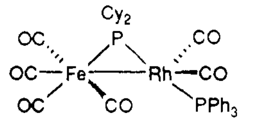

5

but still contain an Fe–Rh bond characterized by downfield chemical shifts for the μ-PCy_2 ligands (**4**, δ 196.6 (ddd); **5**, δ 189.8 (dd)). Complex **4** is the result of simple CO adduct formation at Rh; however, in the presence of excess CO loss of PPh_3 on Fe occurs to produce **5**. These reactions are not immediately reversible upon removal of the CO atmosphere. This is in contrast to a similar reaction for the μ-PPh_2 complexes $(CO)_3(PR_3)Fe(\mu\text{-}PPh_2)Rh(PR_3)(CO)$ (R = Ph, Et), which showed only the reversible formation of a CO adduct similar to **4**.[2] For complexes **4** and **5** the major structural change from **2** is the trans position of the Rh–PPh_3 group. This is presumably a result of increased steric demands at the Rh center, which is now five-coordinate in **4** and **5**.

The reaction of **2** with 1 equiv of PEt_3 results in four products, **6**–**9**, which were identified by $^{31}P\{^1H\}$ NMR. The overall conversion of **2** to products is about 90% with the relative yields of the four products approximately 2:1:2:3 for **6**:**7**:**8**:**9**. All show a downfield chemical shift (**6**, δ 177.4 (dd); **7**, δ 162.2 (dd); **8**, δ 183.9 (ddd); **9**, δ 157.0 (ddd)) attributed to the μ-PCy_2 ligand bridging an Fe–Rh bond, and all remain coordinatively unsaturated at the Rh center in the absence of excess ligand. Complex **9** is the product of simple substitution of PEt_3 for PPh_3 at Rh and can be formulated as $(CO)_3(PPh_3)Fe(\mu\text{-}PCy_2)Rh(PEt_3)(CO)$. This product is easily identified since it is the only product that retains PPh_3 bonded to Fe (δ 80.4 (d)) and shows appropriate coupling of both terminal PR_3 ligands ($^2J_{PP}(Fe)$ = 20.0 Hz and $^2J_{PP}(Rh)$ = 210.9 Hz) to the μ-PCy_2 group. **8** appears to be the product of PEt_3 coordination at Rh with concomitant transfer of CO to Fe and the loss of PPh_3 at Fe, resulting in $(CO)_4Fe(\mu\text{-}PCy_2)Rh(PEt_3)(PPh_3)$. Both PPh_3 and PEt_3 ligands are bonded to Rh as evidenced by $^1J_{PRh}$ coupling (199.1 Hz (PPh_3), 134.9 Hz (PEt_3)) and the $^2J_{PP}$ coupling (29.1 Hz) of these two resonances. The PPh_3 ligand is trans ($^2J_{PP}$ = 212.1 Hz) and the PEt_3

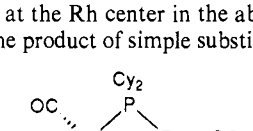

9

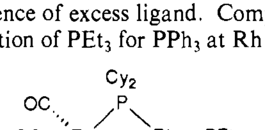

8

---

(29) Breen, M. J.; Geoffroy, G. L. *Organometallics* **1982**, *1*, 1437–1443 and references therein.

(30) Cotton, F. A. *Prog. Inorg. Chem.* **1976**, *21*, 1–28.

(31) Colton, R.; McCormick, M. J. *Coord. Chem. Rev.* **1980**, *31*, 1–52.

(32) Crabtree, R. H.; Lavin, M. *Inorg. Chem.* **1986**, *25*, 805–812.

(33) Horowitz, C.; Shriver, D. *Adv. Organomet. Chem.* **1984**, *23*, 219–305.

(34) Kim. H. P.; Kim, S.; Jacobson, R. A.; Angelici, R. J. *J. Am. Chem. Soc.* **1986**, *108*, 5154–5158.

ligand cis ($^2J_{PP}$ = 14.6 Hz) to the μ-PCy_2 group with the PR_3 ligands distinguished by their relative chemical shifts (δ 30.2 (PPh_3), 8.0 (PEt_3)).

The presence of **6** and **7** in the product mixture is more difficult to rationalize since each is formulated as having five CO groups and this requires a source of CO. It is possible that CO abstraction occurs from some other species in solution, for example, any $Fe(CO)_4PR_3$ that might be present. These two complexes are easily characterized by $^{31}P\{^1H\}$ NMR and by comparison with **2**, **5**, **8**, and **9** and are identified as the complexes $(CO)_4Fe(\mu\text{-}PCy_2)Rh(CO)(PPh_3)$ (**6**) and $(CO)_4Fe(\mu\text{-}PCy_2)Rh(CO)(PEt_3)$ (**7**). Both complexes show a single PR_3 group bound to Rh with $^1J_{PRh}$ (**6**, 136.0 Hz; **7**, 136.8 Hz) and $^2J_{PP}$ indicative of a trans geometry for the phosphorus ligands (**6**, 212.2 Hz; **7**, 214.8 Hz). **6** and **7** are coordinatively unsaturated at Rh, and the change in geometry from a cis arrangement of PPh_3 and μ-PCy_2 in **2** is probably due to decreased steric congestion at adjacent sites on Fe and Rh opposite the PCy_2 bridge.

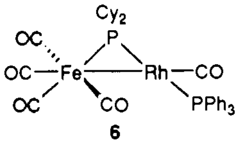

6

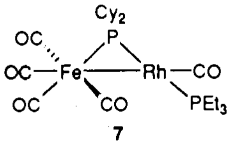

7

The reaction of $(CO)_4Fe(\mu\text{-}PCy_2)Rh(1,5\text{-}COD)$ (**3**) with CO(g) produced three products, **10**–**12**, as evidenced by $^{31}P\{^1H\}$ NMR. Two of these species have a downfield chemical shift (**10**, δ 157.0 (d); **11**, δ 172.9 (d)) indicating retention of the FeRh interaction. However, for the first time we observe an upfield chemical shift (**12**, δ 16.2 (d)), which suggests complete saturation of the coordination sites on both metals, including the loss of the Fe–Rh bond. $^{13}C\{^1H\}$ NMR showed no evidence of coordinated 1,5-COD, so these three products are tentatively formulated as being the result of 1,5-COD displacement and the coordination of one, two, and three CO molecules at Rh to give $(CO)_4Fe(\mu\text{-}PCy_2)Rh(CO)_2$ (**10**), $(CO)_4Fe(\mu\text{-}PCy_2)Rh(CO)_3$ (**11**), and $(CO)_4Fe(\mu\text{-}PCy_2)Rh(CO)_4$ (**12**), respectively.

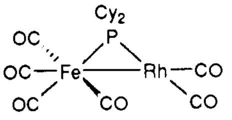

10

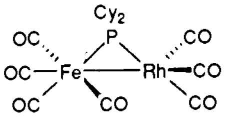

11

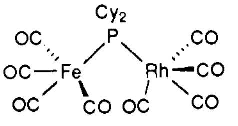

12

Discussion

Coordinatively unsaturated heterobimetallic complexes containing Fe and Rh can be prepared by using the sterically demanding μ-PCy_2 bridging ligand. The observation of a semibridging carbonyl group for **3** in both solution and solid state and for **2** in only the solid state is interesting. However, it is unclear why the solution structure for **2** appears to be anomalous in this type of complex. It is conceivable that, for **2**, a solution process is occurring which rapidly exchanges the Rh–CO group with the Fe–CO ligands, thus preventing direct observation of the semibridging CO group in solution. This process would be less likely for **3**, since **3** contains no CO ligands bound to Rh. The unsaturated nature of these complexes makes exchange processes of this type facile, and the type described here has been observed for other heterobimetallic carbonyl complexes such as $(CO)_3(PEt_3)Fe(\mu\text{-}PPh_2)Rh(PEt_3)(CO)$.[2]

In the case of $(CO)_3Fe(\mu\text{-}PCy_2)Rh(PPh_3)(CO)$ (**2**), for which the μ-PPh_2 analogue is known, it appears that the presence of the more sterically demanding PCy_2 bridging ligand allows for facile dissociation of PPh_3 from Fe evidenced by the formation of $(CO)_4Fe(\mu\text{-}PCy_2)Rh(PPh_3)(CO)_2$ (**4**) under CO(g). This is of course a well-known feature of monometallic complexes containing bulky phosphine ligands. The complex $(CO)_4Fe(\mu\text{-}PCy_2)Rh(1,5\text{-}COD)$ (**3**) is a potential precursor to a variety of related complexes since it contains a readily displaced 1,5-COD ligand. It is also an example of a heterobimetallic complex that undergoes ligand substitution for a donor–acceptor metal–metal bond under mild conditions. The reaction chemistry associated with these complexes is of ongoing interest and will be the subject of further publications.

Acknowledgment. We thank the Natural Sciences and Engineering Research Council of Canada for financial support of this work. The Chemistry Department of the University of Manitoba is gratefully acknowledged for use of their NMR facilities and as the home department of graduate studunt H.A.J.

Registry No. **1**, 113809-78-2; **2**, 119909-51-2; **3**, 119909-59-0; **4**, 119909-52-3; **5**, 119909-53-4; **6**, 119909-54-5; **7**, 119909-55-6; **8**, 119909-56-7; **9**, 119909-57-8; **10**, 119909-60-3; **11**, 119909-61-4; **12**, 119909-58-9; $Fe_2(CO)_9$, 15321-51-4; *trans*-$RhCl(CO)(PPh_3)_2$, 15318-33-9; $[RhCl(1,5\text{-}COD)]_2$, 12092-47-6; Fe, 7439-89-6; Rh, 7440-16-6.

Supplementary Material Available: Tables S-I–S-IV, listing details of the crystallographic investigation, thermal parameters, hydrogen atom positions, and bond distances and angles associated with the cyclohexyl groups (5 pages); Table S-V, listing observed and calculated structure factors (21 pages). Ordering information is given on any current masthead page.

Contribution from the Department of Chemistry and Materials Research Laboratory,
University of Illinois, Urbana, Illinois 61801

Highly Condensed Titanoxanes: Synthesis of *closo*-$(Cp^*Ti)_4O_6$ and Its Transformation to *bicyclo*-$(Cp^*Ti)_4O_5Cl_2$ with $TiCl_4$ as an Oxide Acceptor Reagent

L. M. Babcock and W. G. Klemperer*

Received July 22, 1988

Hydrolysis of Cp^*TiCl_3, $Cp^* = \eta^5\text{-}C_5(CH_3)_5$, under basic conditions yields a titanoxane cage compound, $(Cp^*Ti)_4O_6$ (**1**), having an adamantane-like, tetrahedral Ti_4O_6 core structure. This compound reacts with 0.5 equiv of $TiCl_4$ in toluene solution to form the bicyclic species $(Cp^*Ti)_4O_5Cl$ (**2**) in quantitative yield. Here, one oxygen of the Ti_4O_6 tetrahedron in **1** has been replaced by two terminal chlorine ligands. Compound **2** reacts with $TiCl_4$ unselectively to produce three new compounds, $(Cp^*Ti)_4O_4Cl_4$ (**3**), $(Cp^*Ti)_3O_3Cl_3$ (**4**), and $(Cp^*Ti)_2OCl_4$ (**5**), plus Cp^*TiCl_3. Compound **5** can be isolated from this mixture in analytically pure, crystalline form. Compound **4** can be prepared in high yield from Cp^*TiCl_3 and excess water in acetone solution.

Introduction

The hydrolysis/condensation of titanium(IV) complexes according to eq 1 serves as the basis of many low-temperature route to titania and mixed-metal titanium oxides.[1-3] Although the

$$TiX_4 + 2H_2O = TiO_2 + 4HX \qquad (1)$$

course of this and other sol–gel processes is known to be very

0020-1669/89/1328-2003$01.50/0 © 1989 American Chemical Society